THEORETICAL ANALYSIS OF SUB-WAVELENGTH LIGHT PROPAGATION THROUGH THE DOUBLE-CHAIN SILVER NANORINGS

Y.-F. Chau[*] and W. Y. Yang

Department of Electronic Engineering, Chien Hsin University of Science and Technology, No. 229, Jianxing Rd., Zhongli City, Taoyuan County 32097, Taiwan, R.O.C.

Abstract—Surface plasmon resonance effects on a system consisting of the double-chain silver nanorings are numerically investigated by means of the finite element method with three-dimensional calculations. The numerical results for resonant wavelengths corresponding to different light polarizations, pair numbers, illumination wavelengths, charge distribution and the permittivities filled inside the dielectric holes are reported as well. Results show that the double-chain silver nanorings exhibit tunable plasmon resonances in the near field zone that are not observed for the silver nanodisks of the same volume. The resonance wavelength is redshifted as the filling medium in dielectric holes increases, which is attributed to a longer effective optical path. It can be verified that the proposed structure (e.g., twelve pairs or more pairs) is pertinent to the functionality of long range of wave guiding and also show promise for applications in nanooptical devices, sensing, and surface-enhanced spectroscopy, due to their strong and tunable plasmon resonance.

1. INTRODUCTION

Photonic metal nanoparticles (MNPs) play a crucial role in the emerging field of nanophotonics and plasmonics due to the effects of quantum size and surface plasmon resonance (SPR). The interaction between light and MNPs is dominated by charge-density oscillations on the surface of the MNPs, or localized surface plasmon resonances (LSPRs). These elementary electronic excitations have been the subject of extensive research, both fundamental and the applications

in the design of sensing, biomedicine, imaging, information technology and other optoelectronic devices [1–3]. In such nanostructured pairs, surface plasmon polaritons (SPPs) can be resonantly excited for particular optical wavelengths, depending on the geometrical parameters of the nanostructures as well as on the dielectric function of the metal [4–7]. Plasmonic waveguides of light have been the focus of considerable research lately [7].

These waveguides consist of an array of MNPs with their SPR wavelengths in the region of optical waveguiding. These nanoparticle-structured waveguides hold the unique promise for the light guiding at the nanoscale. For this reason, they are considered very instrumental in the emerging field of nanophotonics where the information transmission and processing occur entirely at the optical level. When a plasmon wave is coupled with a photon at an interface, it is described as SPP, which offers the possibility of transporting energy with light confined below the diffraction limit [5–7] in nanoscale structures. Therefore, employ SPP excitations in the design of nanophotonic devices, such as plasmonic waveguides that involve optical modes at the interface between metallic and dielectric materials, have attracted much interest in recent years [8–10].

From a general point of view, one can envisage using plasmonic devices either by taking advantage of their enhanced local field effects or by propagating the surface plasmons (SPs) over distances large enough to make active integrated devices. For a system with a large number of MNPs, the SPs can become complicated. For example, linear arrays of identical MNPs can yield 5000-fold local-field intensity enhancement [11]. Also, dramatic SP field can be excited at the extremity of finite chains of MNPs [7]. Arrays of MNPs are also used to transport electromagnetic energy in near field regime [12–15].

Several two-dimensional (2-D) studies investigating the propagation of SPP and its confinement within the nanoparticle chain of metallic nanowires (i.e., [10, 11]) have been published to date. However, the mechanism is not clearly discussed in three-dimensional (3-D) model. The resolution provided by the two-dimensional (2-D) model is lower than that expected on the basis of experiments. Of the several possible reasons, the soft decay of the fields in 2D ($r^{-1/2}$ instead of r^{-1}) might be the most fundamental reason. This shows the need for 3-D calculations, which, however, require much computation times. Besides, most of them have focused on the propagation characteristics of single-chain MNPs. Here, we numerically investigate the propagation properties of plasmonic waveguides consisting of the double-chain silver nanoring. A single silver nanoring can be formed by a silver nanodisk with an air-hole or a cylindrical dielectric hole (DH) filling the central part of

the silver nanodisk. The parallel double-chain silver nanorings possess several attractive features which make them interesting as nanoscale optical components. These include tunable optical resonances depending on the dimensions of the air-hole or DH in silver nanorings and the thickness of the metallic shell [16], spanning a large range of frequencies covering the visible and infrared regions of the spectrum [17]. Additionally, nanoshells and other nanoscale metallic structures have been shown to greatly enhance local electromagnetic fields in certain regions near their surfaces at specific wavelengths of light, controlled by the nanostructure geometry [18]. This subwavelength structure can thus be used for manipulating light below the diffraction limit.

In this paper, we investigate the near field response of several-pair arrays of parallel double-chain silver nanorings interacting with an incident plane wave under transverse and longitudinal polarizations by means of finite element method (FEM). We study the effects of pair-pair interaction and the number of pair arrays interaction. The enclosure of several-pair arrays of parallel double-chain silver nanorings forms an open cavity for the electromagnetic field to be effectively confined in the gap and the surface of each pair to generate high local-field enhancement. The number of pair array and the refractive media filled inside the DHs can be varied to tune the near field optical properties and the SPR effects between the MNP pairs. In addition, we compare the optical responses and SPR effects arising from the pair arrays of parallel double-chain silver nanorings with those from the solid silver nanodisks. The effects of wavelength of the incident light, different polarizations of incident light, pattern and number of pair array, charge distribution and the refractive media filled inside the DHs on local-field enhancement will be considered in our simulations.

2. SIMULATION METHOD

Here, two different polarizations of incident light are considered, with the wave vector k along the z-axis and the electric field E perpendicular to the chain axis (z-axis) for the transverse mode, and with k along the x-axis and E parallel to the chain axis (x-axis) for the longitudinal mode, respectively (see the inset of Figure 1(a) and Figure 2). The dispersion properties of the metal (silver) must be considered here since the absorption and permittivity of the metallic material are frequency dependent. Throughout this paper, the silver permittivity data are obtained from Johnson and Christy [19] and fitted to the Drude model [20], with corrections to include the particle size effect [21, 22].

In our simulations, we used 3-D FEM with triangular high order edge elements. To model an infinite simulation region with a 3-

D finite-geometry model (i.e., to enclose the computational domain without affecting the numerical solution), it is necessary to use anisotropic perfectly matched layers (PMLs) that are placed before the outer boundary. This formulation can be used to deal with anisotropic material in terms of both dielectric permittivity and magnetic permeability, allowing anisotropic PMLs to be implemented directly.

3. RESULTS AND DISCUSSION

To start the discussion, consider an array of parallel double-chain of identical MNPs subject to incident optical radiations on its bottom edge (see Figures 1, 2 and 3(a)). At specific wavelengths, this optical incident radiation will excite plasmon resonances in the first MNP which, then through near-field coupling, will induce SPRs in all MNPs that form the chain. This is, in a nutshell, the physical mechanism of light plasmon waveguiding [7]. It is well known that SPRs occur when the wavelength of incident light is large in comparison with MNP dimensions. For this reason, the time–harmonic electromagnetic fields within each MNP and around it vary almost with the same phase. In other words, at any instant of time, the fields locally (around each MNP) look like electrostatic fields.

Firstly, the difference of near field optical performance and SPRs of a pair of silver nanodisk (see the no DH case in the inset of Figure 1(a), where DH means dielectric hole) and a pair of silver nanoring with different permittivities filled inside the DHs (see the DH case in the inset of Figure 1(a)) are investigated. Note that the no DH case is one of the special cases that the DH region is filled with the silver. We compare the SPR behaviors of no DH case with DH cases which are illuminated with transverse polarization of incident wave as shown in the inset of Figure 1. The gap (interparticle spacing) is set to be $w = 20$ nm, the height of nanodisk/nanoring is set to be $t = 10$ nm and the near field intensity is measured at the central part of the MNP pair. Near field intensities of local fields in the central part between two silver nanodisks/nanorings are quite sensitive to the inner radii of the nanorings. On the basis of our simulations [18], we set the radius $R = 50$ nm in no DH case, and the outer and inner radii of $R = 50$ nm and $r = 40$ nm in DH case (i.e., the thickness of silver nanoring is $v = R - r$), respectively. Figure 1(a) shows the near field intensities of no DH case and DH cases as a function of the incident wavelengths with transverse polarization of incident wave. It is well known that the peak wavelength is determined by some factors, i.e., the density of electrons, the electron mass, the size and the shape of the charge distribution.
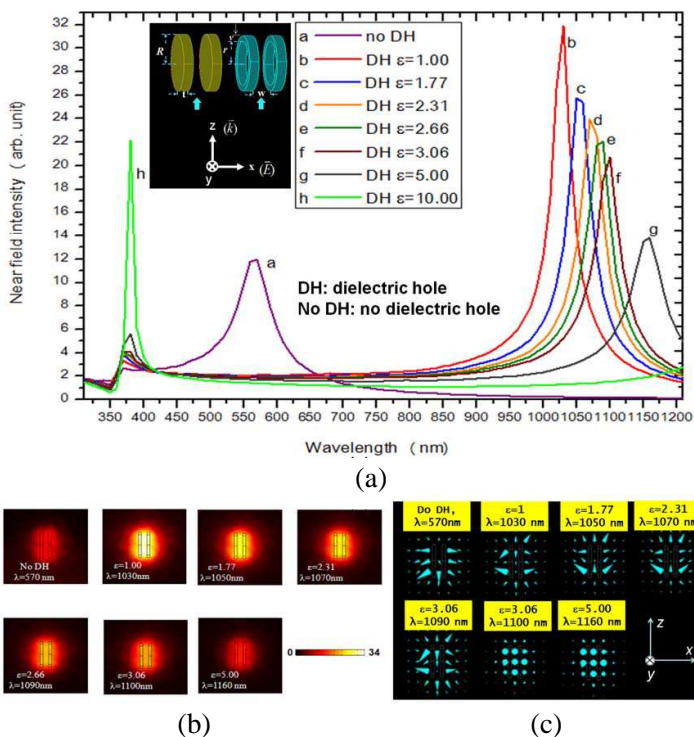
Figure 1. (a) Difference of near field optical response and SPR on a pair of silver nanodisk and a pair of silver nanoring with different permittivities filled inside the DHs under transverse polarization, (b) corresponding TM-mode near-field distributions, and (c) energy flow of a pair of silver nanorings with their corresponding peak wavelengths.

The metal SPRs is the main factor in determining the optical properties of metal MNPs. Many unique optical properties can be achieved when adjusting the structure, morphology, size, nanoshell and composition of the MNPs. In Figure 1(a), it is evident that two clear peak wavelengths for both no DH case and DH cases corresponding to their SPR modes can be found. This phenomenon can be explained by the coupling effects between two MNPs and between MNPs and the incident wave. DHs cases can be considered as truncated circular waveguide. The value of near field intensity measured in the central part of a pair of silver nanoring strongly depends on the permittivities filled inside the DHs, thickness of silver nanoring (i.e., $v = R - r$) and the interparticle spacing (w). Higher refractive media inside the DHs makes the effective

size of DH increasing and increases the effective refractive n_{eff} [18]. As shown in Figure 1(a), when the permittivities filled inside the DHs varying from $\varepsilon = 1$ to $\varepsilon = 5$, the near field intensities are linearly incremental and the maximum SPR mode (peak) is toward longer wavelength. From the DH perturbation, we can express the resonance wavelength shift caused by material perturbation. Thus the increase in permeability $\Delta\mu$ ($= 0$ in this case) or permittivity $\Delta\varepsilon$ of material inside the DH increases the resonance wavelength. The resonance wavelength is redshifted as the filling medium in dielectric holes increases, which is attributed to a longer effective optical path. Note that increasing of the permittivities filled inside the DHs results in a lower field intensity and the red-shift trends with the increasing ε filled inside the DHs, which are good agreement with experiments [23–25]. It is easy to image that the near field intensity is linearly decremented as ε increased due to more incident light is absorbed by higher refractive media in DHs. Their maximum SPR modes (peaks) are also toward longer wavelength as ε increased [26–31]. The apparent corresponding peak resonant wavelengths are $\lambda = 375\,\text{nm}$ (first peak) and $570\,\text{nm}$ (second peak) for no DH case, $\lambda = 380\,\text{nm}$ (first peak) and $\lambda = 1030$–$1160\,\text{nm}$ (second peak) for DH cases as the permittivities filled inside the DHs varying from $\varepsilon = 1$ to $\varepsilon = 5$. By comparing these results with no DH case, it can be observed that the peak resonant wavelengths of DH cases are in the range of near-infrared, which is further shifted to the longer wavelength. Further simulations (the results not shown here) demonstrate that the DH case with higher permittivities filled inside the DHs, would be necessary to resonate at longer wavelength (red-shifted) which means that the SPRs modes can be tuned by varying the permittivities filled inside the DHs.

These results can be attributed to the symmetries of the charge distributions for a pair of silver nanoring with/without DHs. The dipole and quadrupolar (or higher-order) resonance of the silver nanorings could be used to explain the phenomenon of this system. The dipole moments of the inner and outer surfaces of silver nanorings are arranged. A stronger coupling effect could be gotten when the thickness (v) of silver nanorings is much smaller compared with the nanoring radius (r), it will lead to a new scheme of polarization and result in a thin metallic layer, which could be described as symmetric and asymmetric modes [18, 27, 30]. The geometries are air/silver/air gap/silver/air for DH case with $n = 1$, which is very symmetric for the thin silver film, while for another six modes ($n > 1$), the geometry for silver film is asymmetric, i.e., air/silver/DH/silver/air, there will be two independent single-interface modes and not any mode-splitting phenomenon. There are many interfaces between the silver films and

the DHs. It is worth noting the structure of the DH system whose outer environment of a pair of silver nanoring is air. The nanoshell structure is reconciled with the plasmon hybridization model, which was developed by Halas [31] for explaining of the physical origin of the tunable plasmon resonance in silver nanoshells. The nanoshell is a two-surface system, which gets two distinct plasmon modes: an inner shell-surface and an outer shell-surface mode, which couple or hybridize with each other, result in splitting into more new modes. In addition, there are two quadrupolar modes for DH cases, one is at about 380 nm and does not change with permittivities of DHs; others are in the range of 1030–1160 nm with n in the range of 1–5, which seems to liner red-shifted with increasing the permittivities.

The selective corresponding TM-mode near field distributions is depicted in Figure 1(b). For the no DH case, the high local-field enhancement appears in the vicinity of a pair of silver nanodisks and light is well confined effectively between the central part of the nanodisks due to the SPR excitation between the silver nanodisks and the incident light. In contrast to the DH cases, we have another variable ε to explore the near field optical properties in DHs. As can be seen the near field distribution in Figure 1(b), the strong electromagnetic coupling between the inner and outer shell walls when the thickness of silver nanoring is small compared to the outer nanoring radius R. The enhanced intensity in the central gap between a pair of silver nanoring with DHs is due to the SPR and the concentration of energy flow (see Figure 1(c)).

For the DH case, the metal shell thickness ($v = R - r$) represents the distance over which this interaction takes place. The plasmon coupling strength between the core (or cavity) and silver-shell modes vanishes over the shell thickness v similar to the decay of the plasmonic field in the interparticle gap of the particle-pair system. In the silver nanoring system, we can expect the fractional shift of the dipolar resonance to be a function of $(v/r + 1)^{-3}$, where v is the shell thickness and r is the DH radius. In other words, a larger permittivities filled inside the DH has a larger polarizability and a thinner shell ensures stronger near-field coupling, thus leading to a larger fractional plasmon shift. In fact, the dipolar resonance condition for a silver nanoring with DHs structure in the quasistatic limit is specified by [28]:

$$\varepsilon_{DH} = -2\varepsilon_s \frac{\varepsilon_s(1-f) + \varepsilon_m(2+f)}{\varepsilon_s(1+2f) + 2\varepsilon_m(1-f)} \tag{1}$$

where ε_{DH}, ε_s and ε_m are the permittivies of the DH, silver shell, and medium, respectively, and f is the fraction of the volume of the DH in the composite structure. It is interesting to note that f is essentially $[v/r + 1]^{-3}$. This analogy serves to qualitatively explain
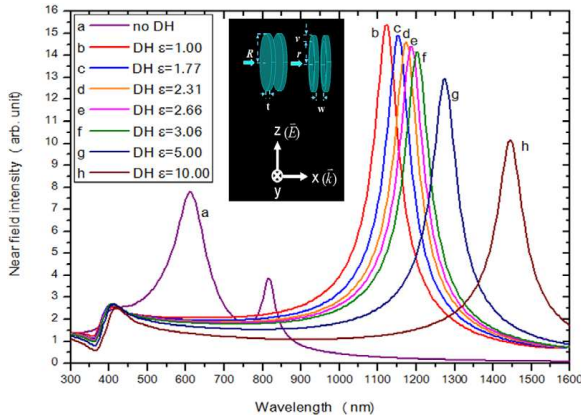
Figure 2. Difference of near field optical response and SPR on a pair of solid silver nanodisk and a pair of silver nanoring with different permittivities filled inside the DHs under longitudinal polarization.

the similarity of the distance dependence and scaling behavior of plasmon coupling in the nanoshell structure to that in the particle-pair structure. Near field coupling between MNPs plays an important role in SPR due to "hot spots" in the resultant electric field (close to the MNPs or in the junction between the MNPs). However, far-field radiation coupling between the MNPs in the array plays also an important role. From the approach used here, it is possible to estimate such a coupling [27, 29].

It is well known that the localized field in the central part of a system consisting of a pair of MNPs is determined by the polarization direction of the incident light [12, 30]. In order to compare the difference on SPRs of two different light polarizations, i.e., the direction of incident wave is perpendicular to the nanochain axis (see the inset of Figure 2, longitudinal polarization) and the direction of incident wave is parallel to the nanochain axis (see the inset of Figure 1(a), transverse polarization). The other parameters are the same as those used in Figure 1(a). As can be seen from the comparison of longitudinal and transverse polarizations, it is evident that transverse polarizations exhibits higher near field intensity in the gap and less red-shifted compared to those of longitudinal polarization. To explain this phenomenon, we can regard the system in Figure 2 (longitudinal polarization, perpendicular to the chain axis) as an open resonant cavity and the system in Figure 1(a) (transverse polarizations, along the chain axis) as a two particles nanochain waveguide. In the waveguide formed by transverse polarizations, energy flows from

first MNP of surface plasmons excited on next one (see Figure 4). Thus, transverse polarizations can provide the direct transmission of propagation light between the particle and particle.

Furthermore, we have performed computations for the case (see Figure 3(a)) of three-pair arrays of double-chain silver nanorings which are illuminated with transverse polarization of incident wave. In these simulations, the direction of the electric field $\mathbf{E}$ is perpendicular to k and parallel to the plane of incidence. Figures 3(b)–(d) compare two cases (no DH and DH cases, see Figure 3(a)) of near field intensities in the central part of three-pair arrays of parallel double-chain silver nanorings as a function of incident wavelengths varied from 305 nm to 1200 nm. The near field intensity is measured at the central part of
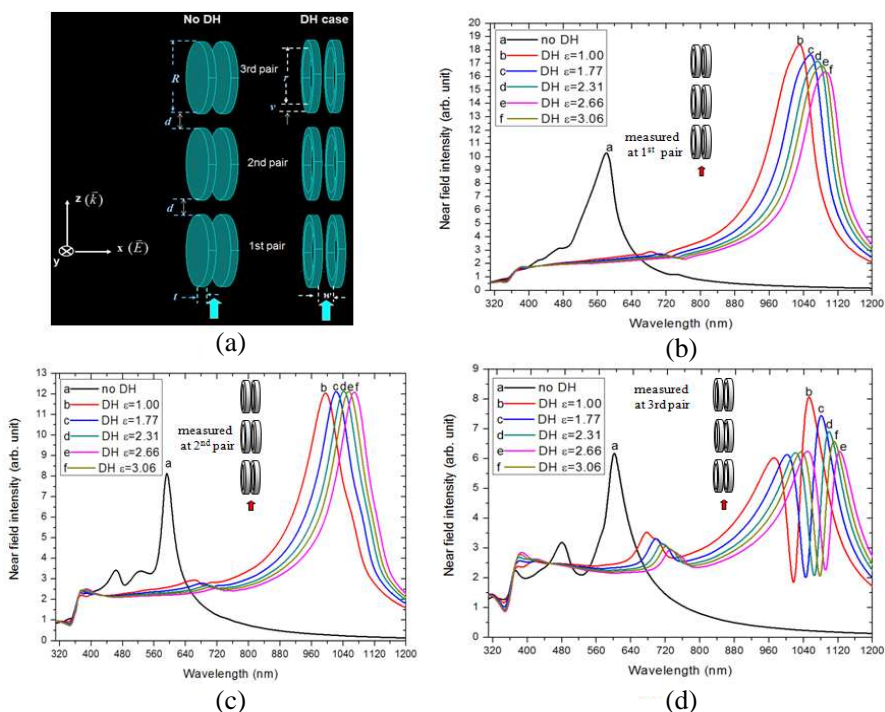

(a)

(b)

(c)

(d)

Figure 3. (a) Schematic of three-pair arrays of double-chain silver nanodisks/nanorings under transverse polarization. Near field intensities of three-pair arrays of silver nanodisks/nanorings as a function of wavelength. The field intensity is measured at the central part of the pair of double chain at (b) 1st pair, (c) 2nd pair and (d) 3rd pair, respectively.

each pair. For no DH case, we have three-pair arrays of parallel double-chain silver nanodisks; and in DH case, we have three-pair arrays of parallel double-chain silver nanorings. For transverse polarization of incident wave, the parameters are fixed as follows: the radius of nanodisk is $R = 50\,\text{nm}$, the inner radius of nanoring is $r = 40\,\text{nm}$, both the interpair distance (d) and the interparticle distance (w) are set to be $20\,\text{nm}$, respectively. As can be seen in Figures 3(b)–(d), DH cases show the same trend as no DH case, except that the peak resonant wavelength shifts to longer wavelengths and the intensities in the central part of each pair become stronger. It can be clearly seen in Figures 3(b)–(d) that the near field intensities of DH cases are higher than those in no DH case within the range of wavelengths close to the peak. As shown in Figure 3(a) that the simulation model of three-pair arrays of double-chain silver nanorings can act as an open cavity system formed by two edges (i.e., 1st and 3rd pairs) and a resonant cavity (2nd pair). When the thickness of the silver-shell ($v = R-r = 10\,\text{nm}$) is near its skin depth (around $10\,\text{nm}$), the near field intensity can be confined on the surface of each silver nanoring and in the gaps between each pair. Note that the strongest local-field enhancement which appears within the MNP gap of each pair is due to LSPR in resonant cavity. The local-field also appears in the gap between two closely spaced pairs because of strong pair-pair interaction. It's unlike the case of single
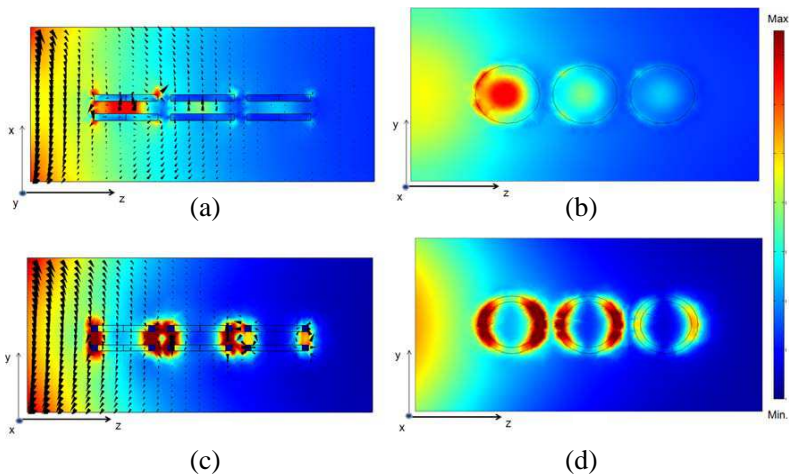

Figure 4. x-z and y-z cross section planes of electrical field distribution measured at the central plane of the three-pair arrays of parallel doulbe-chain MNPs; (a) and (b) for no DH case at $\lambda = 560\,\text{nm}$; (c) and (d) for DH case with $\varepsilon = 1$ at $\lambda = 1000\,\text{nm}$, respectively.

pair system, where the local field usually vanishes in the gap when the direction of the incident electric field is perpendicular to the major axis of the pair. It indicates that the near field intensities in the gaps of three-pair arrays of silver nanorings with DHs can be tuned stronger with a red shift, by varying the permittivities in DHs and the inner radius of nanorings.

Figure 4 shows x-z and y-z cross section planes of electrical field distribution and propagation measured at the central plane of the three-pair arrays of parallel doulbe-chain MNPs; (a) and (b) for no DH case at $\lambda = 560$ nm; (c) and (d) for DH case with $\varepsilon = 1$ at $\lambda = 1000$ nm, respectively. A quit different optical performance can be found between the no DH and DH case, i.e., the field intensity of DH case is much higher than that of no DH case. It is clear to find that the highest symmetry of the electric field intensity and the electrical field between the MNPs differs clearly from those in other region; it also shows that there is a highest electrical field enhancement or called "hot spot" within the MNP gap region, which could be seen in Figure 4.

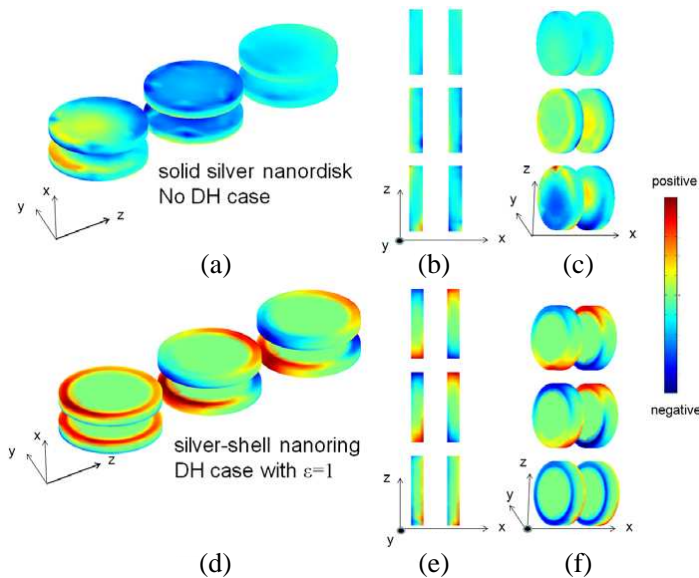Regarding the direction of electric field propagation (black arrows

Figure 5. Different cross section of charge distribution of three-pair arrays of parallel doulbe-chain MNPs, (a) (b) and (c) for no DH case at $\lambda = 560$ nm; (d) (e) and (f) for DH case with $\varepsilon = 1$ at $\lambda = 1000$ nm, respectively.

in Figures 4(a)–4(c)), the schematic charge distributions of no DH and
DH case are also depicted in the Figure 5. Figure 5 shows the different
cross section of charge distribution of three-pair arrays of parallel
double-chain MNPs, for no DH case at $\lambda = 560$ nm, Figures 5(a)–5(c);
for DH case with $\varepsilon = 1$ at $\lambda = 1000$ nm, Figures 5(d)–5(f), respectively.
In no DH case (Figures 5(a)–(c)), the distributed charges on the edge
of surfaces of the silver nanodisk are the same, resulting in SPR mode.
Turning to DH case (see Figures 5(d)–(f)), the distributed charges
on the inner and outer surfaces of the silver nanoring are dipole-like,
leading to a higher field intensity SPR mode. As a result, the radiation
loss in DH case is suppressed, which shows stronger field intensity than
that of DH case. The resonant wavelengths for DH case are shifted to
the longer wavelength as the permittivities of the filling increased.

Finally, the effect of the number of pair arrays on near field
intensity has also been investigated. We further investigate the pair-
pair interactions of different number of pair arrays of silver nanorings
on their local near field enhancement. Figure 6 compares the near
field distribution of six-, eight-, nine- and twelve-pair arrays of parallel
double-chain silver nanorings (DH case, hollow ($\varepsilon = 1$)) with their solid
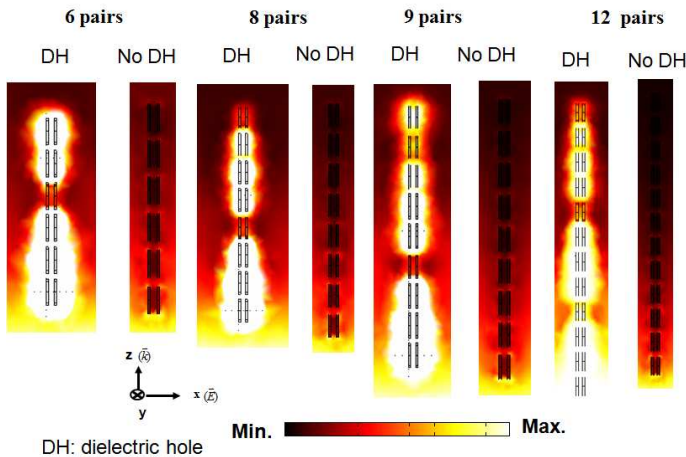cases (no DH cases) at their corresponding peak wavelengths, where

Figure 6. Comparison of the near field distribution of six-, eight-,
nine- and twelve-pair arrays of parallel double-chain silver nanorings
(DH case, hollow ($\varepsilon = 1$)) with their solid cases (no DH cases) at
their corresponding peak wavelengths under transverse polarization of
incident wave, where $\lambda = 560$ nm for no DH case, $\lambda = 1000$ nm for DH
case, respectively.

$\lambda = 560\,\text{nm}$ for no DH case, $\lambda = 1000\,\text{nm}$ for DH case, respectively. The chain waveguides are illuminated with transverse polarization of incident wave. From the field distributions as shown in Figure 6, one can observe that the mesoscopic nature of the finite chain waveguide is clearly visible, as the near field intensity of DH case dramatically enhances the near field intensities within the vicinity of the gap, which exhibit much higher near field intensity than those obtained from no DH cases. It can be verified that the DH case structure (e.g., twelve pairs or more pairs) is pertinent to the functionality of long range of wave guiding or other nanooptical devices, sensing, and surface-enhanced spectroscopy. The field enhancement of the silver nanoring pair originates mainly from the LSPR mode excited by the evanescent field.

4. CONCLUSION AND APPLICATIONS

In conclusion, we have shown that a pair and several-pair arrays of parallel double-chain silver nanorings exhibit tunable SPRs in the near field zone that are not observed for the silver nanodisk pairs of the same volume. The resonance wavelength is redshifted as the filling medium in dielectric holes increases, which is attributed to a longer effective optical path. The volume confined by the arrays of parallel double-chain silver nanorings is filled with refractive medium in DHs and is, therefore, accessible to various sensing and spectroscopy applications at the nanometer scale. As observed from numerical simulations, the main features can be qualitatively understood from simple one-, three-, six-, eight-, nine- and twelve-pair arrays of parallel double-chain silver nanorings and high local field enhancements are generated within the vicinity of the gap of each pair. Such pair arrays of parallel double-chain silver nanorings could serve as resonant nanocavities to hold and probe smaller nanostructures, such as biomolecules or quantum dots. The predictive character of these calculations allows one to tailor the number of pair array or core index of MNP pairs to achieve excitation spectra on demand with a controlled field enhancement and red-shifted resonances. The proposed structures also show promise for applications in nanooptical devices, sensing, and surface-enhanced spectroscopy, due to their strong and tunable plasmon resonance. For example, such a pair arrays of parallel double-chain silver nanorings placed onto a solar cell has the potential to greatly improve the ability of solar cells to harvest light efficiently. For another example, such a structure places into the gain medium of laser resonator can greatly accelerate the speed of population inversion.

ACKNOWLEDGMENT

REFERENCES

1. Lee, K. H., I. Ahmed, R. S. M. Goh, E. H. Khoo, E. P. Li, and T. G. G. Hung, "Implementation of the FDTD method based on Lorentz-Drude dispersive model on GPU for plasmonics applications," *Progress In Electromagnetics Research*, Vol. 116, 441–456, 2011.

2. Liu, X., J. Lin, T. F. Jiang, Z. F. Zhu, Q. Q. Zhan, J. Qian, and S. He, "Surface plasmon properties of hollow AuAg alloyed triangular nanoboxes and its applications in SERS imaging and potential drug delivery," *Progress In Electromagnetic Research*, Vol. 128, 35–53, 2012.

3. Mortazavi, D., A. Z. Kouzani, and K. C. Vernon, "A resonance tunable and durable LSPR nano-particle sensor: Al_2O_3 capped silver nano-disks," *Progress In Electromagnetic Research*, Vol. 130, 429–446, 2012.

4. Koerkamp, K. J. K., S. Enoch, F. B. Segerink, N. F. van Hulst, and L. Kuipers, "Strong influence of hole shape on extraordinary transmission through periodic arrays of subwavelength holes," *Phys. Rev. Lett.*, Vol. 92, 183901, 2004.

5. Raether, H., *Surface Plasmonson Smooth and Rough Surfaces and on Gratings,* Springer-Verlag, Berlin, 1988.

6. Barnes, W. L., A. Dereux, and T. W. Ebbesen, "Surface plasmon subwavelength optics," *Nature*, Vol. 424, 824–830, 2003.

7. Mayergoyz, I. D., "Numerical analysis of nanoparticle-structured plasmon waveguides of light," *IEEE Transactions on Magnetics*, Vol. 43, 1685–1688, 2007.

8. Bozhevolnyi, S. I., J. Erland, K. Leosson, P. M. W. Skovgaard, and J. M. Hvam, "Waveguiding in surface plasmon polariton band gap structures," *Phys. Rev. Lett.*, Vol. 86, 3008–3011, 2001.

9. Saj, W. M., "FDTD simulations of 2D plasmon waveguide on silver nanorods in hexagonal lattice," *Opt. Express*, Vol. 13, 4818–4827, 2005.

10. Chu, H.-S., W.-B. Ewe, E.-P. Li, and R. Vahldieck, "Analysis of sub-wavelength light propagation through long double-chain

nanowires with funnel feeding," *Opt. Express*, Vol. 15, 4216–4223, 2007.

11. Sweatlock, L. A., S. A. Maier, H. A. Atwater, J. J. Penninkhof, and A. Polman, "Highly confined electromagnetic fields in arrays of strongly coupled Ag nanoparticles," *Phys. Rev. B*, Vol. 71, 235408, 2005.

12. Zhia, R., J. A. Schuller, A. Chandran, and M. Brongersma, "Plasmonics: The next chip-scale technology," *Materials Today*, Vol. 9, 20–27, 2006.

13. Maier, S., P. Kik, H. Atwater, S. Meltzer, E. Harel, B. Loel, and A. Requicha, "Local detection of electromagnetic energy transport below the diffraction limit in metal nanoparticle plasmon waveguides," *Nat. Mater.*, Vol. 2, 229–232, 2003.

14. Brongersma, M. L., J. W. Hartman, and H. A. Atwater, "Electromagnetic energy transfer and switching in nanoparticle chain arrays below the diffraction limit," *Phys. Rev. B*, Vol. 62, R16356–R16359, 2000.

15. Maier, S. A., P. G. Kik, and H. A. Atwater, "Optical pulse propagation in metal nanoparticle chain waveguides," *Phys. Rev. B*, Vol. 67, 205402, 2003.

16. Chau, Y.-F., H.-H. Yeh, and D. P. Tsai, "Surface plasmon effects excitation from three-pair arrays of silver-shell nanocylinders," *Phys. of Plasmas*, Vol. 16, 022303, 2009.

17. Baer, R., D. Neuhauser, and S. Weiss, "Enhanced absorption induced by a metallic nanoshell," *Nano Lett.*, Vol. 4, 85–88, 2004.

18. Chau, Y.-F., H.-H. Yeh, and D. P. Tsai, "Near-field optical properties and surface plasmon effects generated by a dielectric hole in a silver-shell nanocylinder pair," *Appl. Optics*, Vol. 47, 5557–5561, 2008.

19. Johnson, P. B. and R. W. Christy, "Optical constants of the noble metals," *Phys. Rev. B*, Vol. 6, 4370–4379, 1972.

20. Okamoto, T., *Near-field Optics and Surface Plasmon Polaritons*, 99, S. Kawata, Ed., Springer, 2001.

21. Ordal, M. A., L. L. Long, R. J. Bell, S. E. Bell, R. R. Bell, R. W. Alexander, Jr., and C. A. Ward, "Optical properties of the metals Al, Co, Au, Fe, Pb, Ni, Pd, Pt, Ag, Ti and W in the infrared and far infrared," *Appl. Optics*, Vol. 22, 4493–4499, 1983.

22. Ordal, M. A., R. J. Bell, R. W. Alexander, Jr., L. L. Long, and M. R. Querry, "Optical properties of the metals Al, Co, Au, Fe, Pb, Ni, Pd, Pt, Ag, Ti, and W in the infrared and far infrared," *Appl. Optics*, Vol. 24, 1099–1120, 1985.

23. Kalele, S., S. W. Gosavi, J. Urban, and S. K. Kulkarni, "Nanoshell particles: Synthesis, properties and applications," *Current Science*, Vol. 91, 1038, 2006.

24. Baida, H., P. Billaud, S. Marhaba, and D. Christofilos, "Quantitative determination of the size dependence of surface plasmon resonance damping in single Ag@SiO2 nanoparticles," *Nano Lett.*, Vol. 9, 3463, 2009.

25. Maceira, V., F. Caruso, and M. Luis, "Coated colloids with tailored optical properties," *J. Phys. Chem. B*, Vol. 107, 10990, 2003.

26. Chen, M. W., Y.-F. Chau, and D. P. Tsai, "Three-dimensional analysis of scattering field interactions and surface plasmon resonance in coupled silver nanospheres," *Plasmonics*, Vol. 3, 157–164, 2008.

27. Ma, Y.-W., J. Zhang, L.-H. Zhang, G.-A. Jian, and S.-F. Wu, "Theoretical analysis the optical properties of multi-coupled silver nanoshell particles," *Plasmonics*, Vol. 6, 705–713, 2011.

28. Chau, Y.-F., H. H. Yeh, and D. P. Tsai, "Surface plasmon resonances effects on different patterns of solid-silver and silver-shell nanocylindrical pairs," *Journal of Electromagnetic Waves and Applications*, Vol. 24, Nos. 8–9, 1005–1014, 2010.

29. Duan, J.-M., X.-F. Lia, L. Yao, S. Pan, and M.-D. Chen, "Local field enhancement of pair arrays of silver nanospheres," *Opt. Commun.*, Vol. 282, 4005–4008, 2009.

30. Chau, Y.-F., H.-Y. Li, Z.-H. Jiang, Y.-F. Chen, C.-S. Lin, M.-S. Liu, F.-L. Wu, and D. P. Tsai, "Manipulation of subwavelength optical fields and resonant field enhancements of a silver-shell nanocylinder pair and chain waveguides with different core-shell patterns," *Journal of Nanoparticle Research*, Vol. 13, 3939–3949, 2011.

31. Prodan, E., C. Radloff, and N. J. Halas, and P. Nordlander, "A hybridization model for the plasmon response of complex nanostructures," *Science*, Vol. 302, 419, 2003.